Peertechz


LIFE SCIENCES GROUP

INTERNATIONAL JOURNAL OF
Veterinary Science and Research

ISSN: 2640-7604 DOI: https://dx.doi.org/10.17352/ijvsr

**Cesar Romero Soares Sousa[1], Ana Luisa Miranda-Vilela[1], Marcos Célio de Almeida[1], Juliana Menezes Soares Fernandes[1], Antonio Sebben[1], Sacha Braun Chaves[1], Kelly Grace Magalhães[1], Caroline Ribeiro da Silva[2], José Luiz Jivago de Paula Rôlo[1], Carolina Madeira Lucci[1], Zulmira Guerrero Marques Lacava[1]**

[1]University of Brasilia, Campus Darcy Ribeiro, Institute of Biological Sciences, Brasília, Brazil, 70.910-900.
[2]Faculty of Medicine, Integrated Faculties of the Planalto Central Educational Union (Faciplac), Campus Gama, DF, Brazil, 72.445-020

**Received:** 28 May, 2019
**Accepted:** 15 July, 2019
**Published:** 16 July, 2019

***Corresponding authors:** Ana Luisa Miranda-Vilela, Department of Genetics and Morphology, Institute of Biological Sciences, University of Brasília, Brasilia, Brazil, Tel: 55 61 3107-3087; Fax +55 61 3107-2923; E-mail: mirandavilela@unb.br

Zulmira Guerrero Marques Lacava, Department of Genetics and Morphology, Institute of Biological Sciences, University of Brasília, Brasilia, Brazil, Tel: 55 61 3107-3087; Fax +55 61 3107-2923; E-mail: zulmira@unb.br

**Keywords:** Immunocompetent animal cancer model; Ehrlich tumor; Orthotopic animal cancer model; Sentinel lymph node; Lymphatic mapping

https://www.peertechz.com

Check for updates

Research Article

# Experimental orthotopic breast cancer as a model for investigation of mechanisms in malignancy and metastasis to the lymph nodes

## Summary

To understand the fundamental mechanisms behind malignancy of breast tumors and also contribute to the discovery of improved methods for prevention, diagnosis and treatment, animal cancer models remain essential. We aimed to establish an optimal orthotopic cancer model for breast cancer in the immunocompetent Swiss mouse, describing the detailed microanatomy of the mammary glands, the sentinel lymph node and lymphatic mapping, evaluating histopathological changes and characterizing the tumor by computed microtomography and interleukins expression. The inoculation of fresh Ehrlich tumor cells led to a detectable tumor as early as 24 hours later; after 7 days, mammary, muscular, dermal vascular and lymphatic invasion were observed and also micrometastases in mammary adipose tissue, sentinel lymph node and contralateral lymph node. From the inoculation site the tumor invaded the host mammary gland structures, the dermis and endomysium of skeletal muscle tissue. Type 1 T helper cytokine levels (IL-1β and IL-17) were significantly higher than anti-inflammatory Type 2 T helper (IL-4) after inoculation of fresh tumor cells. Differently, frozen tumor cells induced tumor development only 14 days after the inoculation while presenting expression of distinct interleukins. The set of findings indicates that orthotopic transplantation provides the microenvironment critical for cell interactions involved in the development of cancer and subsequent metastasis. In this regard, the anatomical and physiological knowledge of the mammary glands and ductal networks favor studies, diagnoses and therapies related to breast cancer and metastasis. Moreover, this study provides anatomical support for the understanding of the lymphatic spread process of cancer cells.

## Introduction

Breast cancer is the second most common type of cancer in all countries and the most common among women, accounting for 25% of all cancers in women and 14% of cancer deaths [1,2]. In spite of the emergence and evolution of new therapeutic approaches over the last half century, such as conservative surgery, chemotherapy, radiotherapy, hormonal therapy and immunotherapy, breast cancer remains the most common cause of cancer deaths among women worldwide [2,3] with an estimated 521,900 cancer deaths and a global increase of 1.7 million new cases diagnosed in 2012 [1]. Thus, early diagnosis of breast cancer is especially important because it enables more effective and less aggressive therapies, may slow disease progression and can lead to a decrease in the mortality rate in breast cancer patients [1,4].

In this regard, axillary lymph node dissection has been accepted for its staging and prognostic value for breast cancer [5]. Further, just as the surgical treatment of breast cancer has evolved from radical mastectomy to breast conserving surgery, surgical treatment of regional lymph nodes has also become less invasive. Lymphatic mapping with sentinel lymph node (SLN) biopsy has contributed to this development, since it has the potential for reducing the morbidity associated with breast carcinoma staging [6-8].

Notwithstanding this progress, to understand the fundamental mechanisms behind malignancy and also contribute to the discovery of improved methods for prevention, diagnosis and treatment, animal cancer models remain essential [9]. In this context, mouse cancer models have been



**Citation:** Soares Sousa CR, Miranda-Vilela AL, de Almeida MC, Soares Fernandes JM, Sebben A, et al. (2019) Experimental Orthotopic Breast Cancer as a Model for Investigation of Mechanisms in Malignancy and Metastasis to the Lymph Nodes. Int J Vet Sci Res 5(2): 046-057. DOI: http://dx.doi.org/10.17352/ijvsr.000041

used successfully, while mouse cancer cells also represent a good model to evaluate the impact of new developments [10,11].

Previous research in modeling cancer in laboratory animals provided new insights into the biology of cancer. Among the existing models, the orthotopic murine is characterized by the transplantation of tumor cells or fragments in the same anatomical site where the tumor was originally developed, or the primary site. This cancer model has been widely used [12,13] and, although complex, favors interactions between the stromal and vascular cells in order to provide a microenvironment that will play a crucial role in the tumor cells' development [14-16].

Currently, the most common animal models used are tumor xenografts in immunodeficient mice [14,17]. However, they fail to model human populations accurately due to important genetic differences between the two species, such as the polymorphism [18]. Thus, an immunocompetent mouse cancer model could help researchers to approximate the use of a more effective model system, even though it still fails to model the human population accurately in this respect.

A wide variety of experimental tumor models has been established for educational and scientific purposes in order to understand the tumor biology better and improve cancer diagnosis and therapeutic strategies [14]. The ascites and solid Ehrlich tumor, originating from a spontaneous breast cancer in female mouse, was used by Apolantem and Ehrlich in 1905 as an experimental tumor model, by transplanting tumor tissues subcutaneously into mice [19,20].

The Ehrlich tumor resembles human tumors; its neoplastic cells are undifferentiated and have a fast growth rate, leading to an increase in chemotherapy sensitivity in mice [19]. This tumor has been used as an experimental model for several different investigations, including antitumor efficiency of photodynamic therapy and magnetohyperthermia [3,21-23] pharmacokinetic studies of chemotherapeutics [24,25] evaluation of tumor growth under effects of *Agaricus blazei*, plant extracts and antioxidants [26]. However, most studies have been conducted using ectopic transplantation into the peritoneal cavity in order to acquire the ascitic tumor, or into the head, femoral region, tongue and footpad, in order to obtain solid tumors [3,21-28].

Therefore, to intentionally develop an optimal animal cancer model either to investigate the fundamental mechanisms in malignancy and metastasis, or to assess the efficacy of novel agents and procedures, this work aimed to establish an orthotopic model for breast cancer using Swiss mice. To meet this goal, detailed microanatomy of the breast, SLN and lymphatic mapping, histopathological description, characterization of the orthotopic tumor transplantation by computed microtomography (CMT), and interleukin dosage in tumor fragments and samples from the contralateral mammary gland were performed. To improve the inoculation procedure, a needle without bevel was used. The tumor model development also involved the optimization of microdissection and staining techniques. Possible systemic impairment was evaluated through hemogram and histological analysis of the heart, liver, kidneys and brain.

## Materials and Methods

### Animals

Non-isogenic female Swiss albino mice, 3-4 months of age and with a body mass of 29.86 ± 0.74 g at the beginning of the experiment, were purchased from the Multidisciplinary Center for Biological Investigation in Laboratory Animal Science (Cemib) of the State University of Campinas (Unicamp, SP/Brazil). Animals were housed in plastic cages (5, 8 or 10/cage, depending on the experiment) at room temperature (20 ± 2 °C) in a 12 h light/dark cycle with lights on at 6 a.m. and free access to food and water.

For the experiments, animals were previously anesthetized by intraperitoneal route using xylazine (10 mg/Kg) and ketamine (80 mg/Kg), in a final dose of 0.1mL/30g. Euthanasia was carried out by cervical dislocation after anesthesia, according to the guidelines on Euthanasia of Federal Council of Veterinary Medicine (CFMV) [29]. All care and procedures were conducted according to the guidelines of the Animal Research Ethics Committee of the University of Brasilia – Institute of Biologic Sciences, Brazil (process nº 44783/2013).

### Identification of the ductal network of the mouse breast

The distribution of the ductal network model was observed employing staining techniques previously described by Krause et al., [30] and Assis et al. (2010) [31], with slight alterations in the microdissection technique. Mice were randomly distributed in two groups (N=5): one group was used as control and the other group injected in the primary duct of the fifth mammary gland with 50 µL of the vital dye Trypan Blue 2% 24 hours before euthanasia.

After euthanasia, breast tissue was removed, fixed in formaldehyde 3.7% NaCl 0.9% in water for 24 hours, dehydrated in alcohol (once in 70%, 80% 90% for 1 hour and 3 times in 100% for 1 hour) and acetone for 72 hours, diaphonized in xylene naphthalene 20% for 72 hours, and finally rehydrated (alcohol 100% 3 times for 1 hour, 90%, 80%, 70% once for 1 hour, and water overnight). For the microdissection procedures, animals were immersed in 0.9% saline solution followed by microsurgical dissecting techniques under a stereoscopic microscope (Steni 2000 Zeiss).

### Ehrlich tumor cells preparation

Ehrlich ascites tumor (EAT) cells were obtained from frozen aliquots maintained in liquid nitrogen and subcultured every week by intraperitoneal (ip) inoculations in mice [27]. EAT cells ($1 \times 10^6$) either fresh or frozen for 30 days at -80º C were used for the orthotopic transplantation. Fresh and frozen EAT cell viabilities were evaluated using Trypan Blue (Sigma) 0.2% staining method followed by counting in a Neubauer chamber [32]. The inoculum concentration ($1 \times 10^6$) was adjusted with phosphate-buffered saline (PBS) to 100 µL.

### Orthotopic transplantation and tumor growth curve

In order to improve the technique of orthotopic transplantation and minimize the occurrence of metastasis



**Citation:** Soares Sousa CR, Miranda-Vilela AL, de Almeida MC, Soares Fernandes JM, Sebben A, et al. (2019) Experimental Orthotopic Breast Cancer as a Model for Investigation of Mechanisms in Malignancy and Metastasis to the Lymph Nodes. Int J Vet Sci Res 5(2): 046-057. DOI: http://dx.doi.org/10.17352/ijvsr.000041

that might occur due to the slightest contact with the needle bevel, or cause transfixation of adjacent anatomical sites, such as muscle and viscera of the abdominal cavity, as well as to restrict the degree of invasiveness of the procedure, the needle (30 cc short needle 8 mm in length and 0.30 mm caliber short 30-gauge BD®) was shortened, thus removing the bevel.

The orthotopic transplantation of tumor cells was modified from Behbod et al., [33]. Ehrlich-solid-tumor-bearing mice were randomly distributed in 10 experimental groups (N= 5 per group), according to fresh (5 groups) or frozen (5 groups) tumor cell use and the time of the tumor analysis, carried out after 1, 2, 7, 14 and 21 days after the inoculation of tumor cells. The negative control group received filtered water and no tumor was implanted.

For the inoculation procedure, anesthetized animals were placed in supine position and observed under stereoscopic microscope. The papilla of the fifth right inguinal mammary gland was clamped and the inoculation needle inserted until a depth of 1 mm directly into the mammary papilla. Subsequently 100 µL ($1 \times 10^6$) of fresh or frozen tumor cells were inoculated into the mammary fat at a 90-degree angle, thus completing the orthotopic transplantation.

Tumors were weighed on an analytical balance (Shimadzu of Brazil, São Paulo) and measured using a digital pachymeter. The tumor volume was calculated according to the formula: length × (width$^2$) × 0.5 mm$^3$ [34]. Data were used to obtain a tumor growth curve.

## Lymphatic mapping and sentinel lymph node (SLN)

Trypan Blue dyeing technique was used to access the lymphatic mapping and thus reveal the SLNs and nodal network, mimicking anatomically and functionally the lymphatic metastatic path of the neoplastic cell from the tumor primary site to the nodal region.

To investigate the occurrence of micrometastasis in SLN, 100 µL ($1 \times 10^6$) of fresh Ehrlich tumor cells were inoculated into the fifth right mammary gland of 34 animals, randomized into 3 groups: control (N = 8) and EAT inoculated animals examined at 7 and 14 days after tumor cell implantation (N = 10/group). Trypan Blue (100 µL) was injected subcutaneously in the subpapillary region on the adipose cushion (subcutaneous mammary papillae), in the 5$^{th}$ right mammary gland and the 4$^{th}$ left mammary gland, 24 hours before euthanasia.

After euthanasia, SLN (right subiliac node) [35,36] was surgically removed, fixed in formaldehyde 3.7% for 8 hours, and processed for histology according to the methodology described above (sections of 2 to 5 m of thickness). Each slide was fitted with a series of three semi-serial sections (50 µm) and stained with hematoxylin-eosin (HE). Sections were photographed under the light microscope Carl Zeiss Axio Vision 4.8.2 SP2, using an image capture Zen System 2011 (Zen blue edition program; Carl Zeiss).

## Histopathological evaluations

Samples from the tumors, the contralateral mammary gland and also from several organs were collected and washed in 0.9% saline solution in order to remove the excess of blood and tissue residues. The liver, kidneys, lung, spleen and brain samples were fixed in formaldehyde 3.7% for 8 hours; the mammary samples were fixed in Davidson solution at 4° C for 8-10 hours. All samples were then processed in an automatic tissue processor (OMA® DM-40, São Paulo, Brazil), cut to 5 µm of thickness with a series of three serial semi-sections (50 µm) in a Leica RM2235 manual microtome (Leica Microsystems, Nussloch, Germany) and stained with HE. The photomicrography of the slides was analyzed by light microscopy (Carl Zeiss Axio Vision 4.8.2 SP2, image capture Zen System 2011 - Zen blue edition program).

## Computed microtomography characterization (CMT)

CMT images of orthotopic tumor were acquired from the anesthetized mouse positioned on a specific small animal scanner of a SkyScan Micro CT 1076 (SkyScan, Kontich, Belgium) operating at 50 kV, 141 mA, with a 0.5 mm aluminum filter. Vital signs were monitored during all the scanning period. Three-dimensional (3D) image reconstruction was performed by Nrecon software (SkyScan, Kontich, Belgium), adjusting the parameters smoothing, beam-hardening and ring-artifact to the values of 01, 10, 07, respectively. For the 3D image evaluation the CTanalyze software (SkyScan, Kontich, Belgium) was used.

## Cytokine profile of mammary glands after orthotopic ehrlich tumor cells inoculation

To investigate whether the orthotopic tumor cells implantation could trigger an immunomodulatory response, the levels of the anti-inflammatory cytokine IL-4 (Th2) and pro-inflammatory cytokines IL-17 (Th1), IL-1β and IL-12p70 (Th1) were evaluated in mammary gland lysates inoculated with fresh and frozen tumor cells using normal mammary glands as control. Because Ehrlich tumor is very aggressive and grows very quickly after the second week, reaching large sizes in short periods [22], cytokines were evaluated at the 14$^{th}$ day after the tumor cell inoculation. For this evaluation, 100 mg of mammary gland was homogenized in lysis buffer (10 mM Tris, pH 7.5, 50 mM NaCl, 1% Triton X-100, 60 mM octyl glucoside) containing protease inhibitors (Boehringer Mannheim). IL-4, IL-17, IL-1β and IL-12p70 levels were measured in mammary gland tissue lysates by enzyme-linked immunosorbent assay (ELISA), in accordance with the manufacturer's instructions (R&D Systems). For each experiment, test and control samples were examined at least in duplicate. Standard curves were prepared with a group of serially diluted standards and used for the calculation of cytokine concentrations.

## Hemogram

Mice were anesthetized with ketamine and xylazine according to the method described above. Blood samples (400 µL) collected by cardiac puncture were used to carry out hemogram in a multiple automated hematology analyzer for veterinary use, Sysmex pocH-100iV Diff (Curitiba/Paraná, Brazil) calibrated for mice in microtubes containing EDTA as anticoagulant.



**Citation:** Soares Sousa CR, Miranda-Vilela AL, de Almeida MC, Soares Fernandes JM, Sebben A, et al. (2019) Experimental Orthotopic Breast Cancer as a Model for Investigation of Mechanisms in Malignancy and Metastasis to the Lymph Nodes. Int J Vet Sci Res 5(2): 046-057. DOI: http://dx.doi.org/10.17352/ijvsr.000041

### Statistical analysis

Statistical analyses were performed using SPSS (Statistical Package for the Social Sciences) version 17.0 (hemogram) or Prism (cytokine profiles) softwares, version 5.0. The continuous variables were tested for normal distribution with the Shapiro-Wilk test. Possible differences between the analyzed groups were investigated by the ANOVA or the Kruskall-Wallis test (when data were not normally distributed); ANOVA followed by the Tukey's test, and Kruskall-Wallis followed by the Mann-Whitney U test (hemogram) or the Dunn's multiple comparison test (cytokine profiles). Values of $p < 0.05$ were considered statistically significant.

## Results

### Characterization of mouse breast and identification of the ductal network

In the female breast of a Swiss mouse were identified five pairs of mammary glands, arranged in two harmonic parallel lines, positioned ventro-laterally, and externalizing the mammary buds surrounded by areola with no coat. Distributed in the cranio-caudal axis, the mammary buds take cervical, thoracic (cranial and caudal), abdominal and inguinal positions (Figure 1a,b). The same ductal network was also observed in mice on the 25$^{th}$ day of lactation (data not shown). The microdissection and histology revealed that the ductal tree of mammary glands is composed of a main duct measuring approximately 3.5 mm in length and 0.51 mm diameter (Figure 1c), which branches into accessory ducts, lobar ducts, lobular ducts, multiple terminal ducts and glandular acini (Figure 1d).

The cervical glands expand cranially towards the submandibular and parotid glands, to occupy the posterior portion of the jaw, with overlap medial and lateral against the level of the throat region. They surround the forelimbs with suprascapular expansion until the medial region and with contralateral overlap in the cervical region (Figure 1a).

The thoracic glands are shown juxtaposed, with laterodorsal projection which progressively narrows in a medial dorsal direction. Abdominal glands expand cranio-caudally and dorso-laterally, overlapping the pair of inguinal glands, which, in turn, expand dorsally, laterally and caudally, surrounding the genital, perineal and perianal regions, with slight lateral subcaudal expansion overlapping contralaterally and ipsilaterally to the abdominal glands (Figure 1b). The glandular tissue below the mammary papilla is made up of a fat pad, parenchyma, stroma, adipose and connective tissues.

Histological sections of mammary gland showed breast parenchyma with ductal and lobular structure without hyperplastic changes. Rare mononuclear cells were present in the lobular stroma (data not showed). The inoculated Ehrlich tumor caused very little antitumor reaction of a cellular nature, but any such reaction was of low intensity and mononuclear. When areas of necrosis were present there was a polymorphonuclear response at the borders of the tumor.

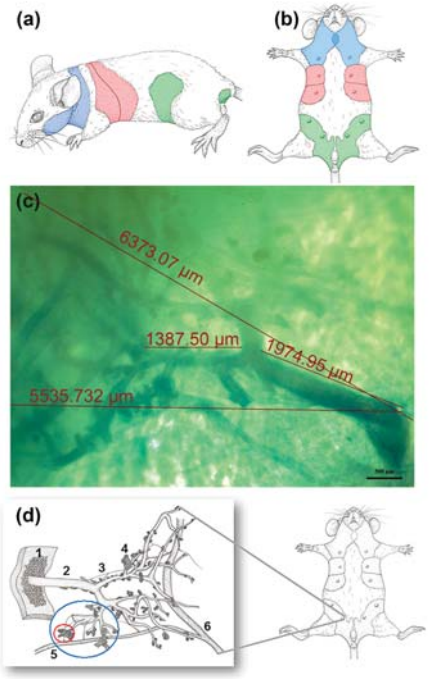


**Figure 1:** Representation and distribution of the mammary glands in Swiss mouse. Mouse in left lateral (a) and supine positions; (b) showing: in blue, pairs of mammary cervical glands overlapping ductal lactiferous area; in pink, two pairs of thoracic mammary glands; and in green, a pair of abdominal mammary glands and a pair of inguinal mammary glands; (c) Measurement of mammary ducts of a Swiss mouse shows main duct measuring approximately 3.5 mm in length and 0.51 mm diameter (scale bars = 500 µm); (d) Illustration of the distribution and details of the mammary gland of Swiss mouse. 1 - fat pad; 2 - Main duct; 3 – capillary; 4 - acini/alveolus; 5 - arteriole; 6 - artery. Red circle: lobule; blue circle: lobe.

### Lymphatic mapping and sentinel lymph node (SLN) of healthy and tumor bearing mouse

The lymphatic and SLN mapping of a healthy control mouse are showed in figure 2. The mammary glands of the negative control group showed no changes and the lymph nodes (LN) were free of tumor involvement. Macroscopically, ipsilateral SLN (right subiliac node) [36], could be viewed in the 4$^{th}$ and 5$^{th}$ mammary glands, lymph vessels, and afferent and efferent blood vessels in the lymph node hilum.

In the group with tumor inoculation of 7 days, positive lymph node involvement with micrometastases was observed in 85% of the animals in ipsilateral SLN (right subiliac node) [36] and contralateral LN (left subiliac node) [36], however, in the group of 14 days, there were metastatic deposits in the right (SLN) and left (contralateral LN) subiliac nodes in 100% and 50% of animals, respectively.

### Characterization of the tumor: Growth curve, histopathology and computed microtomography (CMT)

The inoculation of frozen Ehrlich cells did not induce tumor growth until the 14$^{th}$ day, with little inter-animal variation. However, the tumor growth curve of fresh tumor cells revealed that the tumor development started as soon as 1 day (24 h) after the inoculation and led to high inter-animal variation (Figure 3), as also observed by clinical and histological evaluation. The



**Citation:** Soares Sousa CR, Miranda-Vilela AL, de Almeida MC, Soares Fernandes JM, Sebben A, et al. (2019) Experimental Orthotopic Breast Cancer as a Model for Investigation of Mechanisms in Malignancy and Metastasis to the Lymph Nodes. Int J Vet Sci Res 5(2): 046-057. DOI: http://dx.doi.org/10.17352/ijvsr.000041

growth curve after inoculation of fresh tumor cells showed logarithmic tumor growth from 7 to 14 days, both *in vitro* and *in vivo* (CMT evaluations). During this period metastatic involvement of SLN and LN was detected. Due to these results, the cytokines profiling was performed only 14 days after tumor inoculation.

Histopathological analysis revealed undifferentiated tumors with large necrotic areas invading the host mammary gland, including destruction of ductal structures. The adjacent dermis and skeletal muscle were also infiltrated. Lymphatic vascular invasion was frequently observed inside tumor, peritumoral adjacent mammary tissue, muscle endomysium and dermis after 7 days of tumor inoculation (Figure 4). Micrometastases and overt metastases were identified in the SLN (right subiliac node) and contralateral LN (left subiliac node) [36], after 14 and 21 days (Figure 5). Neurovascular bundle tumor invasion and focal metastases in mammary adipose tissue were rarely observed (data not shown).

The computed microtomography (CMT) of the abdominal wall in the groups inoculated with fresh cells showed the tumor mass (isolated node) with irregular shape and margin in the right inguinal mammary gland, presenting image with a density that matches with the soft parts and isoechogenicity (same texture) of mammary tissue, confirming the tumor implantation after 1 day (24 hours) of tumor inoculation, as well as expansion of the lesion and progressive mass effect (lesion pushing against adjacent structures), particularly at 14 days after inoculation (Figure 6).

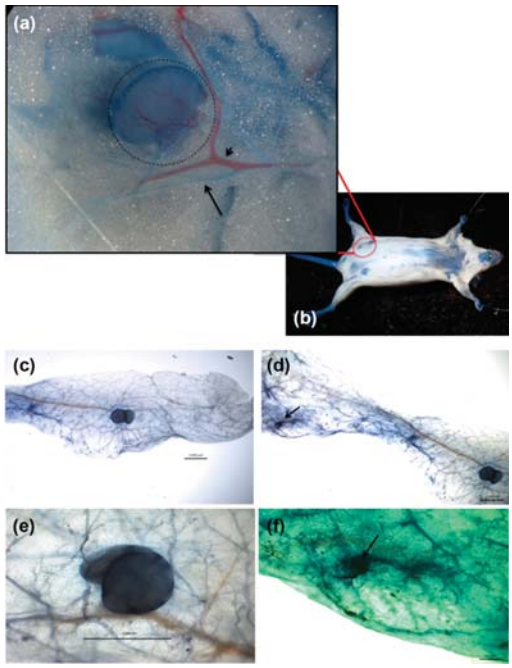


**Figure 2:** Lymphatic Mapping and Sentinel Lymph Node (SLN) of 4th and 5th right normal mammary glands.
(a) The dotted circle indicates the SLN (right subiliac lymph node), the short arrow indicates a blood vessel, and the long arrow, a lymphatic vessel; (b) animal subjected to dyeing technique with vital dye Trypan Blue; (c) SLN (right subiliac lymph node) of the 5th mammary gland; (d) arrow indicates SLN in the 4th mammary gland; (e) detail of the SLN (right subiliac lymph node) of the 5th mammary gland; (f) detail of the figure shown in (d). Scale bars = 2000 μm.

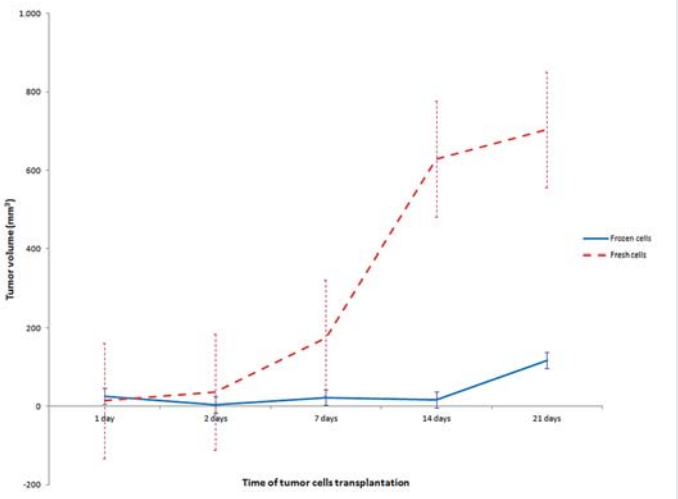


**Figure 3:** Tumor growth curve after orthotopic transplantation of fresh (dashed line) and frozen (solid line) tumor cells.

## Cytokine profile of mammary glands after orthotopic ehrlich tumor cells inoculation

Fresh and frozen tumor cells orthotopically inoculated into the mammary gland triggered different responses in the cytokine profile of mammary glands (Figure 7). The implantation of fresh EAT induced a significant increase in

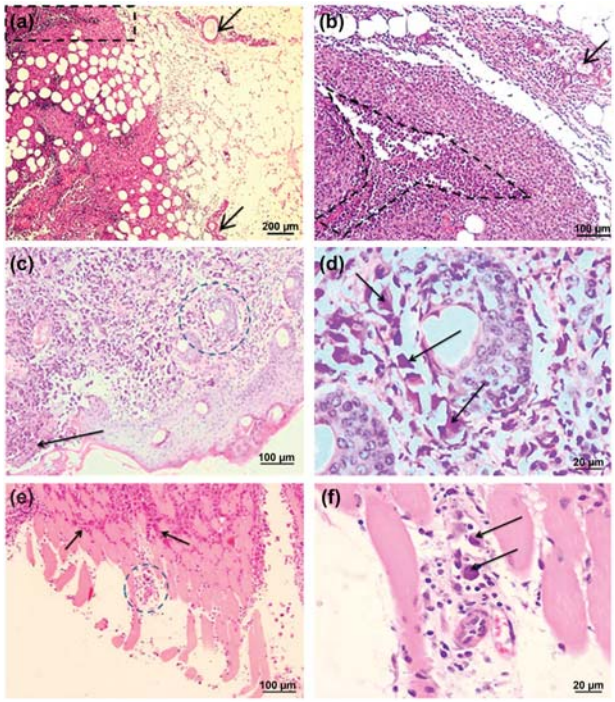


**Figure 4:** Histological characterization of the tumor at 7 days (a-f) after inoculation of fresh tumor cells, showing: (a) Invasive tumor in mammary gland adjacent to a normal area, and normal ductal structures (arrows); (b) Detail of selected rectangular area in Fig. 4a showing invasion frontier, where the dotted line delineates an area of necrosis inside the tumor; normal ductal structures (arrows); (c) Mouse skin showing dermal tumor invasion, with epidermal erosion in the lower left corner of the image (arrow); (d) Details of the circular selected area in Fig. 4c, showing aberrant tumor cells filling a perifollicular lymph vessel (arrows); (e) Extensive endomysial invasion of skeletal muscle (arrows) located below and adjacent to the mammary gland; (f) Details of the selected circular area in Fig. 4e, where a lymph vessel is invaded by tumor cells (arrows).



**Citation:** Soares Sousa CR, Miranda-Vilela AL, de Almeida MC, Soares Fernandes JM, Sebben A, et al. (2019) Experimental Orthotopic Breast Cancer as a Model for Investigation of Mechanisms in Malignancy and Metastasis to the Lymph Nodes. Int J Vet Sci Res 5(2): 046-057. DOI: http://dx.doi.org/10.17352/ijvsr.000041

IL-4 secretion (Figure 7a) and a highly significant increase in IL-1β secretion (Figure 7c), as compared to normal mammary glands (control). This IL-1β secretion was also higher than that observed for frozen cells. Further, the secretion of IL-17 was not significantly changed after fresh cell implantation (Figure 7b). However, the implantation of frozen tumor cells triggered significantly higher IL-17 (Figure 7b) secretion levels than both control and fresh tumor cells inoculated in mammary glands. No detectable levels of IL-12p70 were observed for both fresh and frozen tumor cells implantation (data not shown).

## Histopathological evaluations of organs

No morphological changes were observed in the liver, kidneys, spleen, lung and brain sections at 1, 2, 7, 14 and 21 days after inoculation of EAT cells, as compared to the negative control organs (data not showed).

## Hemogram

Due to the positive lymph node involvement with micrometastases from 7 days after tumor inoculation, results of the hemogram will be presented from this time period (Table 1). Compared to the negative control, fresh and frozen tumor cells at 7 days after inoculation promoted significantly decreased red blood cells (RBC), which were also below the reference values for mice [37,38] with fresh tumor cells. At this time, fresh tumor cells also promoted a significant reduction in hemoglobin (HGB; also below the reference values for mice [37,38] and hematocrit (HCT). Although the tumor did not cause a significant alteration in the absolute number of lymphocytes, its percentage was significantly reduced at all times (7, 14 and 21 days) with fresh tumor cells, the same occurring with frozen tumor cells at 7 and 14 days. Significant increases in the absolute number of neutrophils+monocytes were observed only with fresh tumor cells of 21 days, but non-significant increases occurred in all Ehrlich solid tumor-bearing mice, i.e. both with fresh and frozen tumor cells, and at all times. An increase in the percentage of neutrophils+monocytes was also observed, although this was significant only for fresh tumor cells at 7 and 21 days.

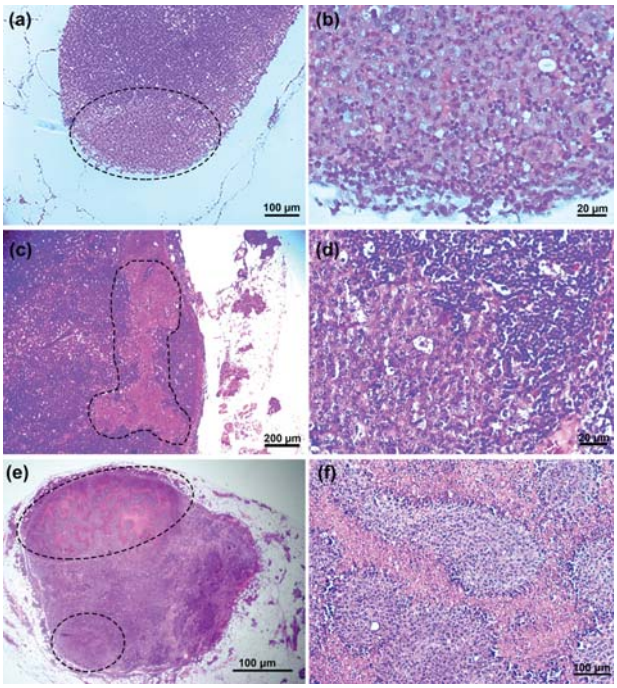


**Figure 5:** Histological characterization of the tumor at 14 days (a-d) and 21 days (e-f) after inoculation of fresh tumor cells, showing: (a) Metastasis in the subcapsular area (selection) of the sentinel lymph node (SLN); (b) Detail of the Fig. 5a revealing a solid group of tumor cells witch present clear nucleolus and marked anisocariose; (c) Sentinel lymph node (SLN) with a metastasis which extends from subcapsular to the cortex of the lymph node (selected area); (d) Detail of Fig. 5c, showing tumor cells bordering the lymph node normal parenchyma; (e) Sentinel lymph node (SLN) showing an overt metastatic lesion (large ellipse) and a small solid micromestastase (small ellipse); (f) Detail of Fig. 5e (selected area inside the large ellipse) evidencing the characteristic pattern of Ehrlich tumor with extensive eosinophilic necrotic areas.

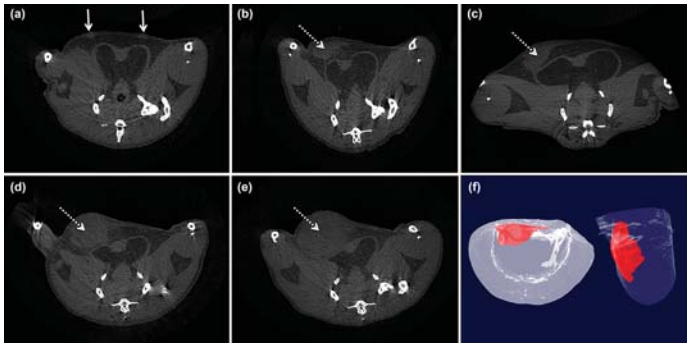


**Figure 6:** Computed microtomography (CMT) of the abdominal wall in the axial plane and bottom view. (a) Control group showing normal mammary glands (solid arrows); (b) nodular image after 1 day (24 hours) of inoculation, showing a lesion of 2.572 × 5.355 mm in the right inguinal mammary gland (dashed arrows) with soft tissue density, shape and irregular margin; (c) nodular image after 7 days of inoculation (dashed arrow) measuring 3.455 mm × 5.435 mm; (d) nodular image after 14 days of inoculation (dashed arrow), showing an expansive lesion of 6.352 mm × 7.355 mm in the right inguinal mammary gland with progressive mass effect (lesion pushing against adjacent structures; (e) nodular image after 21 days (dashed arrow) measuring 7.592 mm × 8.81 mm; (f) tumor 3D image (arrows) after 14 days.

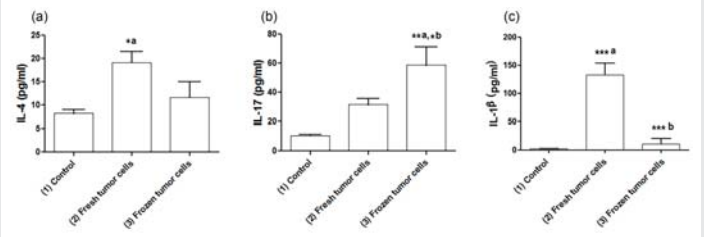


**Figure 7:** Interleukins (Il-4, IL-17 and IL-1ß) dosage in mammary gland lysates evaluated 14 days after inoculation of fresh and frozen Ehrlich tumor cells using normal mammary glands as control. Bar graphics were expressed as mean and SEM (standard error of mean). For IL-4 and IL-17, p-values were generated by ANOVA, while for IL-1β and IL-12p70, p-values were generated by the Kruskall-Wallis test. The superscript letters indicate significant differences detected by the Tukey's or the Dunn's multiple comparison tests, with a= significant compared to control; b=significant compared to fresh tumor cells. Asterisks indicate significant differences at *p<0.05, **p<0.01 and ***p<0.001.

# Discussion

Preclinical cancer studies fall into two main categories: those using tumor cell transplantation, and those in which tumors arise spontaneously or are chemically induced in the host [39]. Although several animal species may be used, the



**Citation:** Soares Sousa CR, Miranda-Vilela AL, de Almeida MC, Soares Fernandes JM, Sebben A, et al. (2019) Experimental Orthotopic Breast Cancer as a Model for Investigation of Mechanisms in Malignancy and Metastasis to the Lymph Nodes. Int J Vet Sci Res 5(2): 046-057. DOI: http://dx.doi.org/10.17352/ijvsr.000041

Table 1: Hemogram of healthy (negative control) and Ehrlich solid tumor-bearing mice at 7, 14 and 21 days after the inoculation of tumor cells.

| | Healthy | Fresh tumor cells | | | Frozen tumor cells | | | p-values |
|---|---|---|---|---|---|---|---|---|
| | Negative control | 7 days | 14 days | 21 days | 7 days | 14 days | 21 days | |
| **Erythrogram** | | | | | | | | |
| **RBC** (x $10^6$/µL) | 8.78 ± 0.42 | 5.33 ± 0.96*a | 8.09 ± 0.39*b | 6.10 ± 1.64 | 6.71 ± 1.01*a | 7.83 ± 0.22 | 6.70 ± 1.34 | 0.097 |
| **HGB** (g/dL) | 11.94 ± 0.45 | 7.43 ± 1.33*a | 11.53 ± 0.58*b | 8.40 ± 2.07 | 9.54 ± 1.40 | 11.26 ± 0.29 | 9.55 ± 1.82 | 0.073 |
| **HCT** (%) | 30.96 ± 1.22 | 19.00 ± 3.33*a | 29.13 ± 1.27*b | 21.43 ± 5.90 | 23.66 ± 3.52 | 28.6 ± 0.78 | 24.83 ± 4.59 | 0.044 |
| **MCV** (fL) | 35.36 ± 0.88 | 35.70 ± 0.19 | 36.00 ± 0.23 | 34.97 ± 0.72 | 36.44 ± 0.53 | 36.52 ± 0.31 | 37.75 ± 1.27 | 0.206 |
| **MCH** (pg) | 13.66 ± 0.49 | 13.80 ± 0.14 | 14.27 ± 0.18 | 14.07 ± 0.64 | 14.22 ± 0.28 | 14.38 ± 0.12 | 14.43 ± 0.36 | 0.600 |
| **MCHC** (g/dL) | 38.60 ± 0.48 | 39.00 ± 0.20 | 39.57 ± 0.34 | 40.30 ± 2.00 | 39.04 ± 0.35 | 39.36 ± 0.15 | 38.23 ± 0.48 | 0.449 |
| **RDW** (%) | 13.66 ± 0.84 | 14.40 ± 0.57 | 13.17 ± 0.12 | 18.97 ± 2.05*b | 13.42 ± 0.54 | 15.00 ± 0.83 | 18.18 ± 5.15 | 0.227 |
| **Leukogram** | | | | | | | | |
| **WBC** (x $10^3$/µL) | 4.94 ± 0.69 | 6.60 ± 1.87 | 3.13 ± 0.72 | 12.70 ± 4.77*a,c | 4.22 ± 0.51 | 2.86 ± 0.44 | 5.48 ± 0.34 | 0.007 |
| **Lymphocytes** (%) | 80.56 ± 3.26 | 33.45 ± 5.13*a | 48.83 ± 5.87*a | 36.03 ± 9.24*a | 58.64 ± 8.70*a | 57.02 ± 5.71*a | 59.08 ± 13.30 | 0.017 |
| **Neutrophils + Monocytes** (%) | 17.82 ± 2.34 | 63.80 ± 5.73*a | 48.03 ± 4.62 | 56.43 ± 10.91*a | 38.66 ± 7.33 | 41.54 ± 5.93 | 39.23 ± 13.72 | 0.009 |
| **Eosinophils** (%) | 1.62 ± 0.98 | 2.75 ± 0.85 | 3.13 ± 1.26 | 7.43 ± 4.81 | 2.70 ± 1.60 | 1.44 ± 0.66 | 1.70 ± 1.27 | 0.383 |
| **Lymphocytes** (x $10^3$/µL) | 4.04 ± 0.65 | 2.20 ± 0.74 | 1.53 ± 0.41 | 3.93 ± 1.53 | 2.32 ± 0.23 | 1.72 ± 0.40 | 3.10 ± 0.59 | 0.065 |
| **Neutrophils + Monocytes** (x $10^3$/µL) | 0.82 ± 0.10 | 4.30 ± 1.25 | 1.50 ± 0.40 | 7.53 ± 3.15*a,c | 1.76 ± 0.49 | 1.12 ± 0.12 | 2.28 ± 0.91*d,≠ | 0.004 |
| **Eosinophils** (x $10^3$/µL) | 0.08 ± 0.04 | 0.10 ± 0.04 | 0.10 ± 0.06 | 1.23 ± 1.04 | 0.14 ± 0.09 | 0.02 ± 0.02 | 0.10 ± 0.07 | 0.288 |
| **Plateletgram** | | | | | | | | |
| **PLT** (x $10^3$/$mm^3$) | 1063.40 ± 271.59 | 856.25 ± 202.21 | 1261.67 ± 75.46 | 965.00 ± 244.39 | 753.28 ± 248.51 | 1211.40 ± 122.56 | 807.69 ± 297.11 | 0.635 |
| **MPV** (fL) | 6.57 ± 0.23 | 6.68 ± 0.22 | 6.45 ± 0.05 | 8.30 ± 0.04 | 6.50 ± 0.35 | 6.46 ± 0.20 | 6.93 ± 0.28 | 0.136 |
| **P-LCR** (%) | 8.13 ± 2.00 | 8.10 ± 1.78 | 7.10 ± 0.30 | 8.40 ± 0.14 | 7.70 ± 2.09 | 8.06 ± 0.89 | 9.48 ± 1.12 | 0.188 |
| **PDW** (fL) | 6.90 ± 0.10 | 6.58 ± 0.05*a | 6.75 ± 0.05 | 8.50 ± 0.10 | 6.74 ± 0.28 | 6.66 ± 0.16 | 7.15 ± 0.18 | 0.138 |

Data were expressed as mean ± SEM (standard error of mean). RBC= red blood cells; HGB= hemoglobin; HCT= hematocrit; MCV= mean corpuscular volume; MCH= mean corpuscular hemoglobin; MCHC= mean corpuscular hemoglobin concentration; RDW = red cell distribution width (represents an indication of the amount of variation – anisocytosis – in cell size); WBC = total white blood cells; PLT= platelet count; MPV= mean platelet volume; P-LCR= platelet large cell ratio; PDW= platelet distribution width; g/dL= grams per deciliter; fl= fentoliters; pg= picograms. P-values of MCV, MCH, MCHC, WBC, Neutrophils + Monocytes (%), Lymphocytes (x $10^3$/µL), Neutrophils + Monocytes (x $10^3$/µL), PLT, MPV and P-LCR were generated by ANOVA, while other p-values were generated by the Kruskal-Wallis test. The superscript letters indicate significant differences detected by Tukey's or the Mann-Whitney U tests, with a= significant compared to negative control; b=significant compared to fresh tumor cells at 7 days; c= significant compared to fresh tumor cells at 14 days; d= significant compared to fresh tumor cells at 21 days. Asterisks indicate significant differences at *p < 0.05 and **p < 0.01. The symbol ≠ indicates significant difference between the comparisons of fresh and frozen tumor cells of same days.

mouse is the most common animal for cancer models [39-41]. In spite of the morphological differences between mouse and human mammary tissue (such as the presence in human mammary tissue of a branching network of ducts ending in clusters of small ductules that constitute the terminal ductal lobular units, and their absence in mouse mammary epithelial tissues, which comprise alveolar buds that are formed during each estrous cycle), significant insights into breast cancer have emphasized functional similarities between them [42]. These similarities, together with easy accessibility, make the mammary gland of mouse the most widely studied organ in improving the understanding of the fundamental cellular and molecular properties of normal and neoplastic development [11,42-45].

Classical tumor diagnostics have for decades been based on surgical pathology and histology, using tumor cell differentiation status as one important aspect to score, evaluate, and communicate tumor aggressiveness. This has prognostic implications where, as a rule, a high degree of differentiation purports a better prognosis than a low degree [46]. As Ehrlich tumor is very poorly differentiated and can morphologically resemble a poorly differentiated or undifferentiated ductal human breast cancer, it can be considered a good model for studying the behavior of this type of aggressive solid cancer. Also, it has the advantage of being successfully used in an immunocompetent mouse cancer model, unlike other established mouse-into-mouse metastatic mammary tumor models, such as 4T1 and EMT6 breast tumor cells, which require syngenetic mice [47]. Another advantage of the Ehrlich tumor cancer model is that it does not require growth in culture medium; it is easily cultivated and transferred in vivo [27].

Although experimental tumor biology has over the years not focused on the differentiation processes, but rather studied molecular pathways leading to growth, migration, and cell death [46], our study aimed for a classical diagnostic approach, since establishing an optimal orthotopic cancer model for breast cancer is the first step in contributing to the translation of basic scientific findings to clinical studies. In this regard, even though a descriptive study and nomenclatorial standardization of the microanatomy and nomenclature of murine lymph nodes has already been reported for BALB/cAnNCrl by Van den Broeck et al. (2006) [36], the detailed microanatomy of the breast and SLN lymphatic mapping, the additional histopathological description and characterization of orthotopic tumor transplantation by computed microtomography (CMT) presented here make this study original and relevant. The



Citation: Soares Sousa CR, Miranda-Vilela AL, de Almeida MC, Soares Fernandes JM, Sebben A, et al. (2019) Experimental Orthotopic Breast Cancer as a Model for Investigation of Mechanisms in Malignancy and Metastasis to the Lymph Nodes. Int J Vet Sci Res 5(2): 046-057. DOI: http://dx.doi.org/10.17352/ijvsr.000041

anatomical and physiological knowledge of the mammary glands and ductal networks favors studies, diagnoses and therapies related to breast cancer and metastasis. Moreover, this study provides anatomical support for the understanding of the lymphatic spread process of cancer cells.

Some reports in the literature have used the orthotopic implantation of tumor cells [12,13,15,16,48]. However, as far as we know, there are no previous studies related to the orthotopic inoculation of Ehrlich tumor. As already mentioned, historically the literature reports many studies performed after ectopic inoculation of the tumor, which is based on transplantation of tumor cells in anatomical sites other than the breast [2,3,21-28,49-57] . However, orthotopic xenografts could more appropriately reproduce the organ environment in which the tumor grows, so that the effect of the tumor on its microenvironment can be modulated [58]. Therefore, the orthotopic tumor transplantation seems to be a better predictor of clinical success than ectopic models, as reported in the literature [59-61].

It is known that the invasiveness generated by surgical orthotopic transplantation significantly increases the likelihood of metastases [62-64] caused by mechanical injuries that may lead even to an increased expression of genes promoting metastasis of breast cancer to the lungs. Furthermore, as reported by the literature data, the orthotopic transplant surgery technique presents limitations, being a highly complicated and invasive procedure, a slow method with high costs, besides causing stress in the animal model [65]. In this respect, our study demonstrated a less invasive and non-surgical orthotopic transplantation of Ehrlich tumor cells to inoculate the tumor cells into the mammary gland. This facilitates the monitoring of the proliferative profile and represents a gain in relation to the surgical orthotopic transplantation, besides allowing clinical and image evaluations, also collaborating in the detection of primary mammary tumor, lymph node staging, evaluation of treatment response, and detection of recurrent and metastatic disease. Moreover, the present protocol facilitates the transplantation procedures, avoiding occurrence of metastasis by the passage of needles with bevel or transfixation to unwanted adjacent anatomic sites, such as muscle, fatty tissue and viscera from the abdominal cavity, reducing discomfort to the animals. Additionally, SLN is defined as the first LN to receive lymphatic drainage from breast cancer, due to the ordered progression of cells through the lymphatic system [66-70]. In view of this, we selected the 5$^{th}$ mammary gland due to the proximity of the right subiliac node [36]. This choice also took into account a reduction in the discomfort of the animals during clinical exams, and facilitated clinical and imaging visualization.

Evaluation of the proliferative profile of the Ehrlich tumor makes it feasible to determine the evolution of this tumor type in its different forms (fresh and frozen cell aliquots), as well as its growth curve. The time of 1 day (24 hours) for the installation of clinical tumor obtained in this study is unprecedented, since the literature reports the clinical appearance of the Ehrlich tumor in its solid form only after 48 hours [322,23,27,71] or even later, as observed for 3 days [72], 7 days [73] and even 12 days [74,75] after ectopic transplantation. In this regard, the earlier clinical detection of the tumor is interesting because it is more suitable for the study of new therapies.

Isolated tumor cells were found in cervical lymph nodes when the Ehrlich tumor was inoculated in mouse tongue, suggesting a metastatic process [76]. Moreover, many human tumors and those transplanted into nude mice have only metastasized when orthotopically inoculated; if held ectopically they often do not metastasize [59,77]). In this regard, the accurate assessment of the SLN, as perfomed in the present study, is important not only for staging and prognosis, but also to guide the treatment selection [78,79], since metastasis to regional LN is an important step in the dissemination of cancer, and often occurs at a relatively early stage of tumor development compared with distant metastasis, such as that to the liver and lung [78].

SLN is the very first lymph node to be reached by metastasing cancer cells coming from the primary tumor site. Indeed SLN is representative of the whole nodal network. Metastases to the SLN are not random, instead following predictable sequential steps. The axillary lymph nodes are the preferred sites for the spread of breast cancer, and the axillary stadium is considered the main prognostic factor, accurately predicting the identification of micrometastases when these cannot be detected by investigatory images. So, it is an important factor in the assessment of prognosis and in decisions about the treatment of breast cancer [6,79,80], and the lymphatic mapping has a great contribution as a diagnostic tool capable of providing regional lymph node status [6,8]. In this respect, as far as we know, observation of micrometastases in Ehrlich tumor in both the ipsilateral SLN (right subiliac node) and contralateral LN (left subiliac node) [35,36] has not previously been described. Actually, in the literature there are no Ehrlich tumor metastasis reports and lymph node involvement. Moreover, for breast cancer, the majority of occurrences are unilateral, with higher tumor incidence on the left. Left-side predominance also occurs in bilateral cases, in which more tumors develop first in the left breast or are larger than those in the right [44]. So, this could explain the rapid metastatic deposits in contralateral LN (left subiliac node) at 7 days after tumor inoculation. However, there was no evidence of metastasis in the several analyzed organs, which may be due to the fact the metastasis searches were performed only until the 21$^{th}$ day. Bioluminescence signals of cells metastasized from the subiliac lymph nodes to the axillary lymph nodes themselves has been described in mutant mice, exhibiting remarkable systemic lymphadenopathy (MRL/lpr) after 3 to 9 days, but were not evident in other organs until the 14$^{th}$ day [78]. Considering our immunocompetent mouse cancer model and the importance, discussed above, of the as-presented non-surgical orthotopic transplantation, a greater length of time than this could be expected to pass before finding metastasis to organs.

It has been reported that several innate cytokines play a crucial role in controlling breast cancer progression. Although much research has focused on the genetic abnormalities that



**Citation:** Soares Sousa CR, Miranda-Vilela AL, de Almeida MC, Soares Fernandes JM, Sebben A, et al. (2019) Experimental Orthotopic Breast Cancer as a Model for Investigation of Mechanisms in Malignancy and Metastasis to the Lymph Nodes. Int J Vet Sci Res 5(2): 046-057. DOI: http://dx.doi.org/10.17352/ijvsr.000041

initiate and drive cancer, there is now overwhelming evidence that the behavior of tumorigenic cells is also highly influenced by their microenvironment [81]. Thus, even though the inoculated Ehrlich tumor caused very little antitumor reaction of a cellular nature, and lymphocyte reaction was rare, results were consistent with those reported in the literature, in which modifications in cytokine profile mediated both directly and indirectly by the tumor are important parameters that affect the course of the disease [81], as discussed below.

Overall, orthotopic tumor cell implantation triggered a polarization towards a pro-inflammatory immune response, since Th1 cytokine secretion levels (IL-1β and IL-17) were significantly higher than anti-inflammatory Th2 (IL-4). IL-4 was originally described as a B cell growth factor, and is now known to provide potent anti-tumor activity against various tumors, including breast cancer [82,83]. Simultaneously, IL-17- and IL-4-producing CD8+ T lymphocytes have been implicated in breast cancer progression, since they have been found within the tumor-draining lymph nodes of breast cancer patients [84]. Likewise, IL-17 secretion has been shown to be up-regulated in breast cancer patients, since it is positively associated with tumor progression aggressiveness [85]. The production of IL-17 in murine models of breast cancer has been described as an important marker of tumor progression [86]. Du and colleagues (2012) [87] showed that injection of 4T1 tumor-bearing mice with recombinant IL-17 resulted in increased tumor volume and microvascular density, as measured by the immunohistochemical detection of CD34 expression in microvessels. IL-1β is another important pro-inflammatory cytokine related to cancer progression. It has been established that IL-1β was predominately responsible for the increased metastatic potential of the tumors [88,89]. In the present study the orthotopic tumor implantation with fresh cancer cells triggered significant amounts of IL-1β, and it could be related with metastasis generation in the analyzed mice.

As the immune system exerts both inhibitory and stimulatory effects on breast tumors, and the balance of these effects may profoundly influence tumor growth [81], the significantly reduced percentage of peripheral lymphocytes at all times (7, 14 and 21 days) with fresh tumor cells, and after 7 and 14 days with frozen tumor cells do corroborate the literature, evidencing that reduced lymphocyte-dependent immunity can favor carcinogenesis [90,91]. Moreover, it has been demonstrated that the development of Ehrlich tumor (both ascites and solid forms) is associated with production of inflammation [27,92], which is in accordance with our results, where tumor cells induced pro-inflammatory cytokines and increased neutrophils+monocytes. This could also be explained by tumor necrosis; the histology is concordant.

Anemia is a common complication in patients with breast cancer, either as a consequence of the disease itself (blood loss, bone marrow infiltration or nutritional deficiencies), or with reduced tumor control or its treatment [93]. Results of erythrogram corroborate this, mainly for fresh tumor cells at 7 days after inoculation. As anemia is a causative factor in the development of tumor hypoxia, which gives rise to a more aggressive tumor phenotype and increased likelihood of distant metastases [93], the aggressiveness of the undifferentiated tumor cells at 7 days with large necrotic areas invading the host mammary gland, destroying ductal structures and infiltrating the adjacent dermis and skeletal muscle, besides the lymphatic vascular invasion, could be explained by anemia.

In conclusion, our study indicates that, with orthotopic inoculation of the Ehrlich tumor, there is a marked invasion of mammary host structures, dermis and muscle associated with vascular lymphatic invasion in these areas. Importantly, micrometastases were frequently seen in the SLN and contralateral LN (left subiliac node). The set of findings indicates that orthotopic transplantation in the microenvironment is critical for cell interactions and subsequent development of cancer and metastasis studies. In this regard, the anatomical and physiological knowledge of the mammary glands and ductal networks favor studies, diagnoses and therapies related to breast cancer and metastasis. Moreover, this study provides anatomical support for the understanding of lymphatic spread in cancer process.

## Acknowledgments

This work was supported by the Brazilian National Council for Technological and Scientific Development (CNPq), the Foundation to Support Research in the Federal District (FAPDF), the Coordination for Further Training of Graduate Staff (CAPES), the CAPES-Network CON-NANO (CAPES), National Institute of Science and Technology in Nanobiotechnology (INCT-Nanobiotecnologia), Center for Nanoscience and Nanobiotechnology of the University of Brasília (CNANO-UnB), and Dean of Research and Post-Graduation of the University of Brasília (DPP-UnB).s

## References

1. ACS (2015) Global Cancer - Facts & Figures., American Cancer Society (ACS), Atlanta 1-61. Link: https://bit.ly/2wC30Xu

2. de Souza AR, Coelho EP, Zyngier SB (2006) Comparison of the anti-neoplastic effects of dirhodium(II) tetrapropionate and its adducts with nicotinate and isonicotinate anions in mice bearing Ehrlich tumors. Eur J Med Chem 41: 1214-1216. Link: https://bit.ly/2XNo1wh

3. Miranda-Vilela A, Yamamoto K, Miranda K, Matos B, Almeida M, et al. (2013a) Dextran-functionalized magnetic fluid mediating magnetohyperthermia for treatment of Ehrlich-solid-tumor-bearing mice: toxicological and histopathological evaluations. Tumour Biol 35: 3391-3403. Link: https://bit.ly/2XLQPde

4. WHO (2007) Early Detection (Cancer control: knowledge into action: WHO guide for effective programmes; module 3.), World Health Organization (WHO), Switzerland. 1-43. Link: http://bit.ly/2Ll0mRV

5. Giuliano AE, Kirgan DM, Guenther JM, Morton DL (1994) Lymphatic mapping and sentinel lymphadenectomy for breast cancer. Ann Surg 220: 391-401. Link: https://bit.ly/32oRkIW

6. Fisher B, Bauer M, Wickerham DL, Redmond CK, Fisher ER, et al. (1983) Relation of Number of Positive Axillary Nodes to the Prognosis of Patients With Primary Breast Cancer. Cancer 52: 1551-1557. Link: https://bit.ly/2LnDRfg

7. Kim T, Giuliano AE, Lyman GH (2006) Lymphatic mapping and sentinel lymph node biopsy in early-stage breast carcinoma: a metaanalysis. Cancer 106: 4-16. Link: https://bit.ly/2XKVJqM



**Citation:** Soares Sousa CR, Miranda-Vilela AL, de Almeida MC, Soares Fernandes JM, Sebben A, et al. (2019) Experimental Orthotopic Breast Cancer as a Model for Investigation of Mechanisms in Malignancy and Metastasis to the Lymph Nodes. Int J Vet Sci Res 5(2): 046-057. DOI: http://dx.doi.org/10.17352/ijvsr.000041

8. Mansel RE, Fallowfield L, Kissin M, Goyal A, Newcombe RG, et al. (2006) Randomized Multicenter Trial of Sentinel Node Biopsy Versus Standard Axillary Treatment in Operable Breast Cancer: The ALMANAC Trial. J Natl Cancer Inst 98: 599-609. Link: https://bit.ly/2ObvpSH

9. Asadishad B, Vossoughi M, Alamzadeh I (2010) *In vitro* release behavior and cytotoxicity of doxorubicin-loaded gold nanoparticles in cancerous cells. Biotechnol Lett 32: 649-654. Link: https://bit.ly/2XTpUaR

10. Chow P (2008) The Rationale for the Use of Animal Models in Biomedical Research. In: Using Animal Models in Biomedical Research: A Primer for the Investigator., P. K. Chow, R. T. Ng and B. E. Ogden, Eds, World Scientific Publishing Company, Singapore. 2-10. Link: http://bit.ly/32kBcrQ

11. Medina D (2010) Of mice and women: A short history of mouse mammary cancer research with an emphasis on the paradigms inspired by the transplantation method. Cold Spring Harb Perspect Biol 2: a004523. Link: https://bit.ly/2GcUaHI

12. Carneiro MLB, Peixoto R, Joanitti G, Oliveira R, Telles L, et al. (2013) Antitumor effect and toxicity of free rhodium (II) citrate and rhodium (II) citrate-loaded maghemite nanoparticles in mice bearing breast cancer. J Nanobiotechnology 11: 4. Link: https://bit.ly/2XSgWum

13. Kubota T (1994) Metastatic models of human cancer xenografted in the nude mouse: the importance of orthotopic transplantation. J Cell Biochem 56: 4-8. Link: https://bit.ly/2SehrO4

14. Vargo-Gogola T, Rosen JM (2007) Modelling breast cancer: one size does not fit all. Nat Rev Cancer 7: 659-672. Link: http://bit.ly/2XKG7ns

15. Witz IP (2009) The Tumor Microenvironment: The Making of a Paradigm. Cancer Microenviron 2: 9–17. Link: http://bit.ly/2GqESiH

16. Witz IP, Levy-Nissenbaum O (2006) The tumor microenvironment in the post-PAGET era. Cancer Lett 242: 1-10. Link: http://bit.ly/2JJlhuG

17. Burgos AE, Belchior JC, Sinisterra RD (2002) Controlled release of rhodium (II) carboxylates and their association complexes with cyclodextrins from hydroxyapatite matrix. Biomaterials 23: 2519-2526. Link: https://bit.ly/32ujEti

18. Sahu SK, Mallick SK, Santra S, Maiti TK, Ghosh SK. et al. (2010) *In vitro* evaluation of folic acid modified carboxymethyl chitosan nanoparticles loaded with doxorubicin for targeted delivery. J Mater Sci Mater Med. Link: http://bit.ly/2Z25m1f

19. Ozaslan M, Karagoz I, Kilic I, Guldur M (2011) Ehrlich ascites carcinoma. Afr J Biotechnol 10: 2375-2378. Link: https://bit.ly/2Sqojbr

20. Silva AE, Santos FGA, Cassali GD (2006) Marcadores de proliferação celular na avaliação do crescimento do tumor sólido e ascítico de Ehrlich. Arq Bras Med Vet Zootec 58: 658-661. Link: http://bit.ly/30x5rdl

21. Chekulayeva L, Shevchuk I, Chekulayev V (2004) Influence of temperature on the efficiency of photodestruction of Ehrlich ascites carcinoma cells sensitized by hematoporphyrin derivative. Exp Oncol 26: 125-139. Link: https://bit.ly/2Obrx47

22. Miranda-Vilela AL, Peixoto RCA, Longo JPF, e Cintra DDOS, Portilho FA, et al. (2013b) Dextran-Functionalized Magnetic Fluid Mediating Magnetohyperthermia Combined with Preventive Antioxidant Pequi-Oil Supplementation: Potential Use Against Cancer. J Biomed Nanotechnol 9: 1261-1271. Link: https://bit.ly/2GcUnuu

23. Portilho FA, Estevanato LLC, Miranda-Vilela AL, Almeida-Santos MFM, de Oliveira-Cavalcanti CE, et al. (2011) Investigation of a magnetohyperthermia system efficacy. J Appl Phys 109: 07B307. Link: http://bit.ly/2JAoj5L

24. Elmorsi YM, El-Haggar SM, Ibrahim OM, Mabrouk MM (2012) Effect of Ketoprofen and Indomethacin on Methotrexate Pharmacokinetics in Mice Plasma and Tumor Tissues. J Appl Pharm Sci 2: 90-95. Link: https://bit.ly/2Sez14q

25. Khanam JA, Salahuddin MS, Habib MR, Islam MR, Jesmin M, et al. (2008) Antineoplastic Activity of Bis-tyrosinediaqua Ni(II) Against Ehrlich Ascites Carcinoma. Dhaka Univ J Pharm Sci 7: 33-37. Link: https://bit.ly/2LkW8K3

26. Verçosa-Junior D, Melo MM, Cassali GD, Dantas-Barros AM, Silva-Junior PGP (2007) Influência de Agaricus blazei Murrill sobre o tumor sólido de Ehrlich e linfonodos poplíteos de camundongos. Arq Bras Med Vet Zootec 59: 150-154. Link: http://bit.ly/2Y9Y4uO

27. Miranda-Vilela AL, Portilho FA, de Araujo VG, Estevanato LL, Mezzomo BP, et al (2011) The protective effects of nutritional antioxidant therapy on Ehrlich solid tumor-bearing mice depend on the type of antioxidant therapy chosen: histology, genotoxicity and hematology evaluations. J Nutr Biochem 22: 1091-1098. Link: https://bit.ly/2Sinp0q

28. Saroja M, Santhi R, Annapoorani S (2012) Antioxidant potential of ethylacetate fraction of cynodon dactylon against ELA implanted swiss albino mice. Int J Pharm Biol Sci 3: 415-419. Link: http://bit.ly/2xPOKxr

29. Conselho Federal de Medicina Veterinária (CFMV) (2013) Guia brasileiro de boas práticas para eutanásia em animais: conceitos e procedimentos recomendados., Comissão de Ética, Bioética e Bem-Estar Animal/CFMV, Brasília/Brazil. 62.

30. Krause S, Brock A, Ingber DE (2013) Intraductal Injection for Localized Drug Delivery to the Mouse Mammary Gland. J Vis Exp 80: 50692. Link: https://bit.ly/2JzmrKE

31. de Assis S, Warri A, Cruz MI, Hilakivi-Clarke L (2010) Changes in mammary gland morphology and breast cancer risk in rats. J Vis Exp 44: 2260. Link: https://bit.ly/2Y6idCe

32. Estevanato L, Cintra D, Baldini N, Portilho F, Barbosa L, et al. (2011) Preliminary biocompatibility investigation of magnetic albumin nanosphere designed as a potential versatile drug delivery system. Int J Nanomedicine 6: 1709-1717. Link: https://bit.ly/2JOa2RY

33. Behbod F, Kittrell F, LaMarca H, Edwards D, Kerbawy S, et al. (2009) An intraductal human-in-mouse transplantation model mimics the subtypes of ductal carcinoma in situ. Breast Cancer Res 11: R66. Link: https://bit.ly/2JNTYzk

34. Dunham SU, Chifotides HT, Mikulski S, Burr AE, Dunbar KR (2005). Covalent binding and interstrand cross-linking of duplex DNA by dirhodium (II,II) carboxylate compounds. Biochemistry 44: 996-1003. Link: https://bit.ly/2JGnS8U

35. Kawashima Y, Sugimura M, Hwang Y, Kudo N (1964) The lymph system in mice. Jap J Vet Res 12: 69-78. Link: https://bit.ly/2LmDhyp

36. Van den Broeck W, Derore A, Simoens P (2006) Anatomy and nomenclature of murine lymph nodes: Descriptive study and nomenclatory standardization in BALB/cAnNCrl mice. J Immunol Methods 312: 12-19. Link: http://bit.ly/2XNp1QN

37. Everds NE (2007) Hematology of the Laboratory Mouse. In: The Mouse in Biomedical Research: Normative Biology, Husbandry, and Models., J. G. Fox, S. W. Barthold, M. T. Davisson, C. E. Newcomer, F. W. Quimby and A. L. Smith, Eds, Vol. III, Elsevier, San Diego, California, USA. 133-170.

38. Thrall MA, Baker DC, Campbell TW, DeNicola D, Fettman MJ, et al. (2007) Hematologia e Bioquímica Clínica Veterinária. Editora Roca, São Paulo, Brazil. 582.

39. Workman P, Aboagye EO, Balkwill F, Balmain A, Bruder G, et al. (2010) Guidelines for the welfare and use of animals in cancer research. Br J Cancer 102: 1555-1577. Link: http://bit.ly/2GdWsX3

40. Andrade A, Pinto SC, Oliveira RS (2002) Animais de Laboratório: criação e experimentação. Fiocruz Rio de Janeiro 388. Link:

41. NIH (2013) BRL Bulletin: NIH Animal Model Resources U. S. D. o. H. a. H. Services, Ed, Vol. 28, National Institutes of Health (NIH), Maryland 1-4.




**Citation:** Soares Sousa CR, Miranda-Vilela AL, de Almeida MC, Soares Fernandes JM, Sebben A, et al. (2019) Experimental Orthotopic Breast Cancer as a Model for Investigation of Mechanisms in Malignancy and Metastasis to the Lymph Nodes. Int J Vet Sci Res 5(2): 046-057. DOI: http://dx.doi.org/10.17352/ijvsr.000041

42. Visvader JE (2009) Keeping abreast of the mammary epithelial hierarchy and breast tumorigenesis. Genes Dev 23: 2563-2577.

43. Murata S, Kominsky SL, Vali M, Zhang Z, Garrett-Mayer E, et al. (2006) Ductal Access for Prevention and Therapy of Mammary Tumors. Cancer Res 66: 638-645. Link: https://bit.ly/2YRLHAM

44. Robichaux JP, Hallett RM, Fuseler JW, Hassell JA, Ramsdell AF (2015) Mammary glands exhibit molecular laterality and undergo left-right asymmetric ductal epithelial growth in MMTV-cNeu mice[ast]. Oncogene 34: 2003-2010. Link: http://bit.ly/2JJjRQS

45. Russo IH, Russo J (1996) Mammary gland neoplasia in long-term rodent studies. Environ Health Perspect 104: 938–967. Link: http://bit.ly/2NVWdWU

46. Jögi A, Vaapil M, Johansson M, Påhlman S (2012) Cancer cell differentiation heterogeneity and aggressive behavior in solid tumors. Ups J Med Sci 117: 217-224. Link: https://bit.ly/2JHZ8gu

47. Fantozzi A, Christofori G (2006) Mouse models of breast cancer metastasis. Breast Cancer Res 8: 212-212. Link: https://bit.ly/32ukCFW

48. Peixoto R, Miranda-Vilela A, Filho J, Carneiro MB, Oliveira RS, et al. (2015) Antitumor effect of free rhodium (II) citrate and rhodium (II) citrate-loaded maghemite nanoparticles on mice bearing breast cancer: a systemic toxicity assay. Tumor Biol 36: 3325-3336. Link: https://bit.ly/2YZ0cDa

49. Aabo K, Vindeløv LL, Spang-Thomsen M (1994) Interaction between three subpopulations of Ehrlich carcinoma in mixed solid tumours in nude mice: evidence of contact domination. Br J Cancer 70: 91-96. Link: https://bit.ly/30wZ8qb

50. Baillif RN (1954) The solid phase of the Ehrlich ascites tumor in mice. Cancer Res 14: 554-558. Link: https://bit.ly/2Y8pu4g

51. Baiochi E, Bigonha JDG, Heymann RE, Feder D, Cabral M, Zyngier SB (1986) Estrógeno em tumor de Ehrlich: estudo da sobrevida e avaliação da resposta imunológica. Arq Méd ABC 9: 22-27. Link: https://bit.ly/2JAkVrz

52. Dale MM (1966) Anaphylactic tests for tumour antigen in transplantable animal tumours. Br J Cancer 20: 326–334. Link: https://bit.ly/2XIH1Rt

53. Lala PK (1972) Age-specific changes in the proliferation of Ehrlich ascites tumor cells grown as solid tumors. Cancer Res 32: 628-636. Link:

54. https://bit.ly/2JI0k3I

55. Möse JR, Möse G (1964) Oncolysis by Clostridia. I. Activity of Clostridium Butyricum (M-55) and Other Nonpathogenic Clostridia against the Ehrlich Carcinoma. Cancer Res 24: 212-216. Link: https://bit.ly/2O5v2IW

56. Sugiura K (1953) Effect of Various Compounds on the Ehrlich Ascites Carcinoma. Cancer Res 13: 431-441. Link: http://bit.ly/2JCj4Tf

57. Takeuchi J (1967) Effect of intraperitoneal and subcutaneous injection of chondroitin sulphate on the growth of solid Ehrlich ascites tumour. Br J Cancer 21: 334-337. Link: https://go.nature.com/2NVWXLG

58. Tannock IF (1969) A comparison of cell proliferation parameters in solid and ascites Ehrlich tumors. Cancer Res 29: 1527-1534. Link: http://bit.ly/30EU3wl

59. Richmond A, Su Y (2008) Mouse xenograft models vs GEM models for human cancer therapeutics. Dis Model Mech 1: 78–82. Link: http://bit.ly/2JI2uA6

60. Hoffman RM (1999) Orthotopic metastatic mouse models for anticancer drug discovery and evaluation: a bridge to the clinic. Invest New Drugs 17: 343-359. Link: https://bit.ly/2GcvYoI

61. Killion J, Radinsky R, Fidler I (1998) Orthotopic Models are Necessary to Predict Therapy of Transplantable Tumors in Mice. Cancer Metastasis Rev 17: 279-284. Link: https://bit.ly/2JGpwY8

62. Kuo TH, Kubota T, Watanabe M, Furukawa T, Kase S, et al. (1993) Site-specific chemosensitivity of human small-cell lung carcinoma growing orthotopically compared to subcutaneously in SCID mice: the importance of orthotopic models to obtain relevant drug evaluation data. Anticancer Res 13: 627-630. Link: https://bit.ly/2Y4vw5T

63. Al-Sahaf M, Lim E (2015) The association between surgical volume, survival and quality of care. J Thorac Dis S152-S155. Link: https://bit.ly/2GfxEh9

64. Kocatürk B, Versteeg HH (2015) Orthotopic Injection of Breast Cancer Cells into the Mammary Fat Pad of Mice to Study Tumor Growth. J Vis Exp 96: 51967. Link: https://bit.ly/2Gdo8v3

65. Rashid OM, Nagahashi M, Ramachandran S, Graham L, Yamada A, et al. (2013) Resection of the primary tumor improves survival in metastatic breast cancer by reducing overall tumor burden. Surgery 153: 771-778. Link: http://bit.ly/2Y59e4b

66. Bibby MC (2004) Orthotopic models of cancer for preclinical drug evaluation: advantages and disadvantages. Eur J Cancer 40: 852-857. Link: https://bit.ly/2LnBwRw

67. Coelho-Oliveira A, Rocha ACP, Gutfilen B, Pessoa MCP, Fonseca LMBD (2004) Identificação do linfonodo sentinela no câncer de mama com injeção subdérmica periareolar em quatro pontos do radiofármaco. Radiol Bras 37: 233-237. Link: https://bit.ly/30x9Kp3

68. Morton DL, Wen D, Wong JH (1992) Technical details of intraoperative lymphatic mapping for early stage melanoma. Arch Surg 127: 392-399. Link: https://bit.ly/32vhSIr

69. Quadros LGDA, Gebrim LH (2007) A pesquisa do linfonodo sentinela para o câncer de mama na prática clínica do ginecologista brasileiro. Rev Bras Ginecol Obstet 29: 158-164. Link: http://bit.ly/2NV29z8

70. Sado HN, Graf RM, Timi JRR, Urban CA, Yamada AS, et al. (2008) Linfonodo sentinela após mamoplastia de aumento pela via transaxilar: estudo prospectivo controlado por meio de linfocintilografia em 43 pacientes. Radiol Bras 41: 283-288. Link: http://bit.ly/2Shhl8e

71. Urban CDA, Lima RSD, Schünemann Júnior E, Hakim Neto CA, Yamada A, et al. (2001) Linfonodo sentinela: um novo conceito no tratamento cirúrgico do câncer de mama. Rev Col Bras Cir 28: 216-222. Link: http://bit.ly/2XTeUdb

72. Miranda-Vilela AL, Grisolia CK, Longo JPF, Peixoto RCA, de Almeida MC, et al. (2014) Oil rich in carotenoids instead of vitamins C and E as a better option to reduce doxorubicin-induced damage to normal cells of Ehrlich tumor-bearing mice: hematological, toxicological and histopathological evaluations. J Nutr Biochem 25: 1161-1176. Link: https://bit.ly/2JMRS2T

73. Sadeghiani N, Guedes M, Oliveira D, Tedesco A, Lima E, et al. (2006) Effects of Magnetic Field and Magnetoliposomes on Mice: Cytotoxicity and Genotoxicity Tests. Magnetics, IEEE Transactions on. 42: 3605 - 3607. Link: http://bit.ly/2Y3fauA

74. Sakai M, Fonseca ESM, Oloris SCS, Matsuzaki P, Otake AH, et al. (2006) Effects of peripheral-type benzodiazepine receptor ligands on Ehrlich tumor cell proliferation. Eur J Pharmacol 550: 8-14. Link: http://bit.ly/2YRtYtr

75. Abdel-Rahman MN, Kabel AM (2012) Comparative study between the effect of methotrexate and valproic acid on solid Ehrlich tumour. J Egypt Natl Canc Inst 24: 161-167. Link: https://bit.ly/2xNUXKl

76. Kabel AM (2014) Effect of Combination between Methotrexate and Histone Deacetylase Inhibitors on Transplantable Tumor Model. Am J Med Studies 2: 12-18. Link: https://bit.ly/2XSbOpS

77. Bicalho LS, Longo JP, Cavalcanti CE, Simioni AR, Bocca AL, et al. (2013) Photodynamic therapy leads to complete remission of tongue tumors and inhibits metastases to regional lymph nodes. J Biomed Nanotechnol 9: 811-818. Link: https://bit.ly/2NSL2hx

78. Glinskii AB, Smith BA, Jiang P, Li XM, Yang M, et al. (2003) Viable circulating metastatic cells produced in orthotopic but not ectopic prostate cancer models. Cancer Res 63: 4239-4243. Link: https://bit.ly/2xPHZMg




**Citation:** Soares Sousa CR, Miranda-Vilela AL, de Almeida MC, Soares Fernandes JM, Sebben A, et al. (2019) Experimental Orthotopic Breast Cancer as a Model for Investigation of Mechanisms in Malignancy and Metastasis to the Lymph Nodes. Int J Vet Sci Res 5(2): 046-057. DOI: http://dx.doi.org/10.17352/ijvsr.000041

79. Li L, Mori S, Sakamoto M, Takahashi S, Kodama T (2013) Mouse Model of Lymph Node Metastasis via Afferent Lymphatic Vessels for Development of Imaging Modalities. PLoS ONE 8: e55797. Link: https://bit.ly/2xPxzMw

80. Lyman GH, Temin S, Edge SB, Newman LA, Turner RR, et al. (2014) Sentinel Lymph Node Biopsy for Patients With Early-Stage Breast Cancer: American Society of Clinical Oncology Clinical Practice Guideline Update. J Clin Oncol 32: 1365-1383. Link: https://bit.ly/2Y6jzwG

81. Pitorre M, Bastiat G, dit Chatel Elodie M, Benoit JP (2015) Passive and specific targeting of lymph nodes: the influence of the administration route. Eur J Nanomed 7121. Link: http://bit.ly/32CUs4a

82. Korkaya H, Liu S, Wicha MS (2011) Breast cancer stem cells, cytokine networks, and the tumor microenvironment. J Clin Invest 121: 3804-3809. Link: https://bit.ly/2JVj93l

83. Jia X, Yu F, Wang J, Iwanowycz S, Saaoud F, et al. (2014) Emodin suppresses pulmonary metastasis of breast cancer accompanied with decreased macrophage recruitment and M2 polarization in the lungs. Breast Cancer Res Treat 148: 291-302. Link: https://bit.ly/2XK9ENT

84. Nagai S, Toi M (2000) Interleukin-4 and breast cancer. Breast Cancer 7: 181-186. Link: https://bit.ly/2Y3dWzu

85. Faghih Z, Rezaeifard S, Safaei A, Ghaderi A, Erfani N (2013) IL-17 and IL-4 producing CD8+ T cells in tumor draining lymph nodes of breast cancer patients: positive association with tumor progression. Iran J Immunol 10: 193-204. Link: https://bit.ly/2Y1zSe5

86. Benevides L, Cardoso CRB, Tiezzi DG, Marana HRC, Andrade JM, Silva JS (2013) Enrichment of regulatory T cells in invasive breast tumor correlates with the upregulation of IL-17A expression and invasiveness of the tumor. Eur J Immunol 43: 1518-1528. Link: https://bit.ly/2YWNEfm

87. Zhang X, Weng W, Xu W, Wang Y, Yu W, et al. (2014) Prognostic significance of interleukin 17 in cancer: a meta-analysis. Int J Clin Exp Med 7: 3258-3269. Link: http://bit.ly/2JMdmg3

88. Du JW, Xu KY, Fang LY, Qi XL (2012) Interleukin-17, produced by lymphocytes, promotes tumor growth and angiogenesis in a mouse model of breast cancer. Mol Med Rep 6: 1099-1102. Link: https://bit.ly/2JzizJC

89. Saijo Y, Tanaka M, Miki M, Usui K, Suzuki T, et al. (2002) Proinflammatory Cytokine IL-1β Promotes Tumor Growth of Lewis Lung Carcinoma by Induction of Angiogenic Factors: In Vivo Analysis of Tumor-Stromal Interaction. J Immunol 169: 469-475. Link: http://bit.ly/2YThxxh

90. Voronov E, Shouval DS, Krelin Y, Cagnano E, Benharroch D, et al. (2003) IL-1 is required for tumor invasiveness and angiogenesis. Proc Natl Acad Sci USA. 100: 2645-2650. Link: http://bit.ly/2XKcxOJ

91. Ames BN, Shigenaga MK Hagen TM (1993) Oxidants, antioxidants, and the degenerative diseases of aging. Proc Natl Acad Sci USA. 90: 7915-7922. Link: https://bit.ly/2QI1qyc

92. Miranda-Vilela AL, Peixoto RCA, Longo JPF, e Cintra DDOS, Portilho FA, et al. (2013c) Dextran-Functionalized Magnetic Fluid Mediating Magnetohyperthermia Combined with Preventive Antioxidant Pequi-Oil Supplementation: Potential Use Against Cancer. J Biomed Nanotechnol 9: 1261-1271. Link: https://bit.ly/2GcUnuu

93. Sun Y, Colburn NH, Oberley LW (1993) Depression of catalase gene expression after immortalization and transformation of mouse liver cells. Carcinogenesis 14: 1505-1510. Link: http://bit.ly/2YSj0nf

94. Leonard RC, Untch M, Von Koch F (2005) Management of anaemia in patients with breast cancer: role of epoetin. Ann Oncol 16: 817-824. Link: https://bit.ly/2SgnMIO






**Citation:** Soares Sousa CR, Miranda-Vilela AL, de Almeida MC, Soares Fernandes JM, Sebben A, et al. (2019) Experimental Orthotopic Breast Cancer as a Model for Investigation of Mechanisms in Malignancy and Metastasis to the Lymph Nodes. Int J Vet Sci Res 5(2): 046-057. DOI: http://dx.doi.org/10.17352/ijvsr.000041